Supporting Information

Oxygen Atom Transfer Promoted Nitrate to Nitric Oxide Transformation: A Step-wise Reduction of Nitrate → Nitrite → Nitric Oxide

Kulbir,[†] Sandip Das,[†] Tarali Devi,[ǁ] Mahesh Yenuganti,[†] Mrigaraj Goswami,[†] Somnath Ghosh,[†] Subash Chandra Sahoob,[‡] Pankaj Kumar*[†]

[†]Department of Chemistry, Indian Institute of Science Education and Research (IISER), Tirupati 517507, India

[ǁ]Humboldt-Universität zu Berlin, Institut für Chemie, Brook-Taylor-Straße 2, D-12489 Berlin, Germany

[‡]Department of Chemistry, Punjab University, Punjab, Chandigarh, India

* To whom correspondence should be addressed.

E-mail: pankaj@iisertirupati.ac.in

Table of Contents

Materials: All reagents and solvents obtained from commercial sources (Sigma Aldrich Chemical Co. and Tokyo Chemical Industry) were of the best available purity and used without further purification unless otherwise indicated. Solvents were dried according to reported literature and distilled under an inert atmosphere before use.[S1] $Na^{15}NO_2$ and $Na^{15}NO_3$ (99.2% 15N-enriched) were purchased from ICON Services Inc. (Summit, NJ, USA). The 12-TMC ligand was prepared by reacting excess amounts of formaldehyde and formic acid with 1,4,7,10-tetraazacyclododecane as reported previously.[S2]

Instrumentation: UV-vis spectra were recorded on a Hewlett-Packard 8453 diode array spectrometer equipped with a thermostat cell holder (UNISOKU Scientific Instruments) designed for low-temperature experiments. FT-IR spectra in solid form were recorded on Bruker-Alpha Eco-ATR FTIR spectrometer using the standard KBr disk method. ^{1}H-NMR spectra were measured with a Bruker model Ascend 400 FT-NMR spectrometer. Electrospray ionization mass spectra (ESI-MS) were recorded on an Agilent Mass Spectrometer (6200 series TOF/6500 series Q-TOF B.08.00) by infusing samples directly into the source using a manual method. The spray voltage was set at 4.2 kV and the capillary temperature at 80 °C. GC-MS analyses were recorded on an Agilent 7890B GC system equipped with a 5977B MSD Mass analyzer.

Synthesis of [(12-TMC)Co^{II}(ACN)]$(BF_4)_2$ (1). CH_3CN solution (5 mL) of Cobalt(II) tetrafluoroborate hexahydrate (409 mg, 1.2 mmol) was added to 12-TMC (229 mg, 1 mmol) CH_3CN solution of with constant stirring followed by refluxed for 12 hours at 80 ºC. During this color of the solution changed to wine red after reaction completion. The reaction mixture was dried over vacuum and then washed with cold methanol several times to remove excess $[Co^{II}(H_2O)_6](BF_4)_2$. Diethyl ether (50 mL) was added to precipitate out complex **1** (wine red solid). The precipitate was collected and dried under vacuum over anhydrous $CaCl_2$. To get X-ray quality single crystals, the solid was re-dissolved in CH_3CN layered with diethyl ether and kept at -20 °C; after two days, dark brown colored crystals were obtained. Yield: 425 mg (~ 85%). UV: λ_{max} = 485 nm (ε = 170 M^{-1} cm^{-1}). FT-IR (KBr pellet): 2925, 1635, 1475, 1084, 755 cm^{-1}. Mass (*m/z*): Calcd*:* 374.2, Found: 374.2.

Synthesis of [(12-TMC)Co^{II}(NO_3)](BF_4) (2): To a 20 ml CH_3CN solution of [(12-TMC)Co^{II}(ACN)]$(BF_4)_2$ (502 mg, 1 mmol), 1 mL aqueous solution of $NaNO_3$ (85 mg, 1 mmol) was added slowly with constant stirring. The mixture was stirred for one hour at RT (298 K) until the color of the solution changed from wine red to light pink, indicating completion of the reaction. The volume of the reaction mixture was decreased to 10 mL over rotary vacuum and

then layered with diethyl ether and kept for crystallization at -20 °C. Yield: 400 mg (~ 90%). UV: λ_{max} = 472 nm (ε = 25 M^{-1} cm^{-1}). FT-IR (KBr pellet): 2925, 1384, 1084, 755 cm^{-1}. Mass (m/z): Calcd: 349.1, Found: 349.1. [(12-TMC)Co^{II}($^{15}NO_3$)](BF_4) (**2**-$^{15}NO_3^-$) was prepared by using the same method with $Na^{15}NO_3$. FT-IR (KBr pellet): 2925, 1358, 1084, 755 cm^{-1}. Mass (m/z): Calcd: 350.1, Found: 350.1

Synthesis of [(12-TMC)Co^{II}(NO_2)](BF_4) (3). To a 20 ml CH_3CN solution of [(12-TMC)Co^{II}(ACN)](BF_4)$_2$ (502 mg, 1 mmol), 1 mL aqueous solution of $NaNO_2$ (69 mg, 1 mmol) was added slowly with constant stirring. The mixture was stirred for one hour at RT (298 K) until the color of the solution changed from wine red to pink, indicating completion of the reaction. The volume of the reaction mixture was decreased to 10 mL over rotary vacuum and then layered with diethyl ether and kept for crystallization at -20 °C. Yield: 350 mg (~ 85%). UV: λ_{max} = 535 nm (ε = 24 M^{-1} cm^{-1}). FT-IR (KBr pellet): 2925, 1271, 1084, 755 cm^{-1}. Mass (*m/z*): Calcd*:* 333.1, Found: 333.1. [(12-TMC)Co^{II}($^{15}NO_2$)](BF_4) was prepared using the same method with $Na^{15}NO_2$. FT-IR (KBr pellet): 2925, 1245, 1084, 755 cm^{-1}. Mass (*m/z*): Calcd*:* 334.2, Found: 334.2.

Synthesis of {CoNO}^{8} (4). The Ar saturated CH_3CN solution (10 mL) of [(12-TMC)Co^{II}](BF_4)$_2$ (0.461 g, 1 mmol) was purged with an excess of NO for 5 min; and the color of the solution was changed from light pink to wine red color. The reaction mixture was kept for 30 min, and excess of NO was removed with Ar (degassing) and then layered with Ar saturated ether. Deep wine red colored crystals [(12-TMC)Co^{III}(NO)] (BF_4)$_2$ were obtained by slow diffusion after several days at -20 °C. UV: λ_{max} = 370 nm (ε = 800 M^{-1} cm^{-1}). FT-IR (KBr pellet): 2925, 1703, 1084 cm^{-1}. Mass (*m/z*): Calcd: 404.2, Found: 404.2 ([(12-TMC)Co^{III}(NO)(BF_4)]$^+$). ^{1}H-NMR: active (Figure S6e).

Reactivity Studies: All UV-vis spectral measurements were run in a UV cuvette in H_2O at RT. All kinetic reactions were run at least three times, and the data reported here are the average outcome for these reactions. We have performed all the reactions using H_2O as solvent at room temp (298 K). The formation of **4** and $VOCl_3$ in the reactions was identified by comparing with authentic samples, and product yields were calculated by comparing with standard curves prepared with original samples.

^{15}N-labeling Experiments by FT-IR Spectroscopy: we have recorded the IR spectra of the different complexes in their solid form as KBr pellet to follow the source of nitrogen. The IR spectra of complex **2** showed a nitrate ($^{14}NO_3^-$) characteristic peak at 1384 cm^{-1}, which

shifted to 1358 cm^{-1} when prepared with ^{15}N-labeled nitrate ($^{15}NO_3^-$). The change in the IR stretching frequency of cobalt bound nitrate (Δ = 26 cm^{-1}) confirmed that an increase in the reduced mass of nitrogen atom (^{14}N to ^{15}N) is responsible for the decrease in the stretching frequency of the nitrate functional group. Similarly, the IR spectra of complex **3** showed a nitrite ($^{14}NO_2^-$) characteristic peak at 1271 cm^{-1}, which shifted to 1245 cm^{-1} when prepared with ^{15}N-labeled nitrite ($^{15}NO_2^-$). The change in the IR stretching frequency of cobalt-bound nitrite (Δ = 26 cm^{-1}) confirmed that an increase in the reduced mass of nitrogen atom (^{14}N to ^{15}N) is responsible for the decrease in the stretching frequency of the nitrate functional group. We observed similar spectral changes when the IR spectra of cobalt bound nitrosyl complex recorded with ^{14}N and ^{15}N-labeled cobalt nitrosyl complexes. The IR spectra of **4** showed a characteristic nitrosyl stretching frequency at 1703 cm^{-1} (^{14}N), which shifted to 1673 cm^{-1} (^{15}N, Δ = 30 cm^{-1}) when exchanged with ^{15}N-labeled nitrosyl functional group.

Nitrate Reduction and Nitrite Reduction ^{15}N-labeling Experiments by ESI-Mass Spectrometry: To establish the source of nitrogen, complex **2** and **3** with ^{15}N-labeled nitrate and nitrite were reacted with 2.2 equiv. and 1 equiv. of VCl_3 in H_2O at 298 K, respectively. The reaction mixture was kept for one hour, and then ESI mass spectra of the reaction mixture were recorded.

Reactivity of [(12-TMC)$Co^{II}(NO_3)](BF_4$) (2) + VCl_3: Complex **2** was reacted with excess VCl_3 in H_2O to confirm the reaction product of nitrate reduction reaction. The color of the above reaction mixture changed to wine red from pink over a period of one hour, indicating the formation of **4**. The end product, obtained in the reaction of **2** and VCl_3, was determined to be $\{Co(NO)\}^8$ from various spectroscopic and structural characterization. To grow good crystals for X-ray data, the red product was reacted with sodium tetraphenylborate to give a deep red solid in MeOH (changed counter anion). The deep wine red colored crystals were obtained by keeping the solution layered with Et_2O at -20 °C for 3 days. UV: λ_{max} = 370 nm (ε = 760 M^{-1} cm^{-1}). FT-IR (KBr pellet): 2925, 1703, 1100, 1077 cm^{-1}. Mass (m/z): Calcd: 404.2, Found: 404.2 ([(12-TMC)$Co^{III}(NO)(BF_4)]^+$)

Reaction of [(12-TMC)$Co^{II}(NO_2)](BF_4$) (3) + 1 equivalent VCl_3: Complex **3** was reacted with 1 equivalent amount of VCl_3 in H_2O to confirm the reaction product of NO_2^- reduction reaction. To confirm the end product, **3** was reacted with 1 equivalent of VCl_3 in H_2O at RT. The color of the above reaction mixture changed to red from light pink upon the addition of 1 equivalent VCl_3 over a period of 3-5 minutes, indicating the formation of **4**. The end product, obtained in the reaction of **3** and VCl_3, was determined to be $\{Co(NO)\}^8$ from various

spectroscopic and structural characterization. To grow good crystals for X-ray data, the red product was reacted with sodium tetraphenylborate to give a deep red solid in MeOH (changed counter anion). The deep red colored crystals were obtained by keeping the solution layered with Et_2O at -20 °C for 3 days. UV: λ_{max} = 370 nm (ε = 760 M^{-1} cm^{-1}). FT-IR (KBr pellet): 2925, 1703, 1100, 1077 cm^{-1}. Mass (m/z): Calcd: 404.2, Found: 404.2 ([(12-TMC)Co^{III}(NO)(BF_4)]$^+$).

Magnetic moment calculation and determination of the number of unpaired electrons in complex 2:

Evans' method of ^{1}H-NMR was performed to determine the number of unpaired electrons (spin state) in complex **2** at room temperature (298K). A WILMAD® coaxial insert (with a sealed capillary) tube containing the only CD_3CN solvent (with 1.0% TMS) was inserted into the normal NMR tubes containing the complex **2** (4.0 mM, with 0.1% TMS). We have calculated the chemical shift value of the TMS peak in the presence of complex **2** with respect to that of the TMS peak in the outer NMR tube. The magnetic moment was calculated using the given equation,

$$\mu_{eff} = 0.0618(\Delta\nu T / 2fM)^{1/2}$$

$$\mu_{eff} = 0.0618 * (56 * 298 / 2 * 400 * 0.004)^{1/2}$$

$$\mu_{eff} = 4.46 \text{ BM}$$

Where f = oscillator frequency (MHz) of the superconducting spectrometer, T = absolute temperature, M = molar concentration of the complex **2**, and ν = difference in frequency (Hz) between the two TMS signals.[S3, S4, S5] The calculated magnetic moment of complex **2** was determined to be 4.46 BM in CD_3CN at RT, suggesting 3 unpaired electrons in the Co^{2+} center of complex **2**.

Calculation of Binding Constant(K_b): The binding constants, K_b(Co^{II}-NO_3^-), K_b(Co^{II}-NO_2^-) & K_b(Co^{II}-NO), were determined by titrating the complex **1** with respect to the different concentrations of NO_3^-, NO_2^- & NO, respectively. The stock solutions of **1** (5.0 mM & 2.50 mM) were prepared in CH_3CN and the guest solutions were prepared in the required solvents in 5.0 mM ($NaNO_3$ and $NaNO_2$ in H_2O-CH_3CN in 1:9 v/v) & 14 mM ($NO_{(g)}$ in CH_3CN), respectively. Solutions of **1** with increasing concentration of the guest molecules were prepared separately. The UV-vis spectra of these solutions were recorded by means to get absorbance values. The binding constants were calculated using the Benesi-Hildebrand equation.[S6, S7] K_b was calculated from the equation stated below.

$$1/(A\text{-}A_o) = 1/\{K_b(A_{max}–A_o)\,[X]_n\} + 1/[A_{max}\text{-}A_o]$$

Here, A_o is the absorbance of **1** in the absence of guests, A is the absorbance in the presence of guests at different concentration, A_{max} is the absorbance in the presence of added $[X]_{max}$ where X was NO_3^-, NO_2^-, and NO, respectively, and K_b is the binding constant (M^{-1}). The binding constants (K_b) were determined from the slope of the straight line of the plot of 1/(A-Ao) against 1/(Amax–Ao)$[X]_n$. The binding constant (K_b) as determined by UV-vis titration method for **2**, $K_b(Co^{II}\text{-}NO_3^-)$, **3**, $K_b(Co^{II}\text{-}NO_2^-)$, **4**, K_b ($\{CoNO\}^8$) with X is found to be 2.3×10^2 M^{-1}, 2.5×10^3 M^{-1} & 2.4×10^3 M^{-1} for NO_3^-, NO_2^- and NO, respectively

Detection of 4 by ^{1}H-NMR. To confirm the **4** formations in the reaction of **2** with 2.2 fold VCl_3, we have monitored the reaction by ^{1}H-NMR spectroscopy. The ^{1}H-NMR spectrum of complex **2** (1.04 mg / 600 μL, 4 mM) with 2.2eq, 1.eq, 0.2eq of VCl_3 in CD_3OD showed signals at 3.68, 3.20, and 2.43 ppm, corresponds to a 12-TMC ligand which was absent in **2** and compared with the authentic $\{CoNO\}^8$ samples (Figure S10). Additionally, we have calculated the amount of formation of **4** by comparing peak integral at 3.68 ppm of the reaction mixture (**2** + VCl_3) with the authentic sample **4** containing an internal standard Benzene (7.35 ppm; Figure S10).

S. No.	Sample	Integral of benzene peak (7.37 ppm) (A)	Integral of 12-TMC peak (3.68 ppm) (B)	Ratio (B) / (A)
1	$[(12\text{-TMC})Co^{III}(NO)]^+$	6	8	1.33
2	**2** + 2.2 equiv. VCl_3	6	7.2	1.20
3	**2** + 2.2 equiv. VCl_3	6	7.46	1.24
4	**2** + 2.2 equiv. VCl_3	6	7.3	1.21

<u>Amount of {Co-NO}^{8} formed:</u>

Sample 1 = (1.20 / 1.33) × 4 mM = 3.6 mM (90 %)

Sample 2 = (1.24 / 1.33) × 4 mM = 3.72 mM (93 %)

Sample 3 = (1.21 / 1.33) × 4 mM = 3.63 mM (90.7 %)

4 formed in the reaction (average): = ~ 91.23 %

Single-Crystal XRD Studies. Crystals were mounted on Hampton cryoloops. All geometric and intensity data for the crystals were collected using a Super-Nova (Mo) X-ray diffractometer equipped with a micro-focus sealed X-ray tube Mo-Kα (λ = 0.71073 Å) X-ray source and HyPix3000 (CCD plate) detector of with increasing ω (width of 0.3 per frame) at a scan speed of either 5 or 10 s/frame. The CrysAlisPro software was used for data acquisition and data extraction. Using Olex2[S8], the structure was solved with the SIR2004[S9] structure solution program using Direct Methods and refined with the ShelXL[S10] refinement package using Least Squares minimization. All non-hydrogen atoms were refined with anisotropic thermal parameters. Few anions, mainly BF_4 ions, were found to be highly disordered, and an appropriate disordered model was applied (Figure S4 and S11). Detail crystallographic data and structural refinement parameters are summarized in Table T1 - T4. CCDC 2058407 (**2**), 2058406 (**4**), contains the supplementary crystallographic data for this paper. These data can be obtained free of charge from The Cambridge Crystallographic Data Centre.

References

S1. W. L. Armarego, *Purification of laboratory chemicals*, Butterworth-Heinemann, **2017**.

S2. J. A. Halfen, V. G. Young, Jr., *Chem. Commun.,* **2003**, 2894-2895.

S3. D. F. Evans, *J. Chem. Soc.*, **1959**, 2003-2005.

S4. S. Das, Kulbir, S. Ghosh, S. Chandra Sahoo, P. Kumar, *Chemical Science,* **2020**, *11*, 5037-5042

S5. M. Yenuganti, S. Das, Kulbir, S. Ghosh, P. Bhardwaj, S. S. Pawar, S. C. Sahoo, P. Kumar, *Inorganic Chemistry Frontiers*, **2020**, *7*, 4872-4882.

S6. S. Goswami, D. Sen, N. K. Das, H. K. Fun, C. K. Quah, *Chem Commun (Camb)*, **2011**, *47*, 9101-9103.

S7. J. Chen, H. Yoon, Y. M. Lee, M. S. Seo, R. Sarangi, S. Fukuzumi, W. Nam, *Chem Sci*, **2015**, *6*, 3624-3632;

S8. Dolomanov, O. V.; Bourhis, L. J.; Gildea, R. J.; Howard, J. A. K.; Puschmann, H., OLEX2: a complete structure solution, refinement and analysis program. *J Appl Crystallogr* **2009,** *42*, 339-341

S9. Burla, M. C.; Caliandro, R.; Camalli, M.; Carrozzini, B.; Cascarano, G. L.; De Caro, L.; Giacovazzo, C.; Polidori, G.; Siliqi, D.; Spagna, R., IL MILIONE: a suite of computer programs for crystal structure solution of proteins. *J Appl Crystallogr* **2007,** *40*, 609-613

S10. Sheldrick, G. M., Crystal structure refinement with SHELXL. *Acta Crystallogr C Struct Chem* **2015,** *71*, 3-8

Table T1 Crystallographic data for **2** and **4**.

	2	**4**
Chemical formula	$C_{36}H_{48}BCoN_5O_3$	$C_{61}H_{68}B_2CoN_5O_2$
Formula weight	668.53	955.79
Wavelength /Å	0.71073	0.71073
Crystal system	monoclinic	monoclinic
Space group	$P2_1/c$	Ia
T, K	140	140
a, Å	14.66223(19)	17.5811(3)
b, Å	9.57975(12)	32.4018(4)
c, Å	23.8521(4)	18.2337(2)
α, °	90	90
β, °	95.9041(12)	90.6880(10)
γ, °	90	90
V/ $Å^3$	3332.51(8)	10386.2(2)
Z	4	4
Calculated density, g/cm^3	1.332	1.248
Abs. Coeff. $/mm^{-1}$	0.559	0.378
Reflections collected	39091	4148.0
Unique reflections	7122	71166
Refinement method	Least-squares on F^2	Least-squares on F^2
Data/restraints/parameters	7122/0/419	20067/2/1288
Goodness-of-fit on F^2	1.055	1.098
Final *R* indices [$I > 2\sigma(I)$]	$R_1 = 0.0317$	$R_1 = 0.0833$,
	$wR_2 = 0.0800$	$wR_2 = 0.2133$
R indices (all data)	$R_1 = 0.0377$	$R_1 = 0.0955$,
	$wR_2 = 0.0831$	$wR_2 = 0.2258$

Table T2 Selected bond lengths (Å) and bond angles (°) for **2** and **4.**

2		**4**	
Co1 O1	2.1712(11)	Co1 N1	1.975(5)
Co1 O2	2.1610(12)	Co1 N2	1.988(6)
Co1 N1	2.1820(13)	Co1 N3	1.981(5)
Co1 N2	2.2206(13)	Co1 N4	1.984(6)
Co1 N3	2.1501(12)	Co1 N5	1.773(6)
Co1 N4	2.2078(12)		
O1 Co1 N4	132.83(4)	N3 Co1 N2	87.6(2)
O1 Co1 N2	91.03(4)	N3 Co1 N4	87.1(2)
O1 Co1 N1	131.18(5)	N1 Co1 N3	155.7(2)
O2 Co1 O1	59.11(4)	N1 Co1 N2	87.1(2)
O2 Co1 N4	92.38(5)	N1 Co1 N4	88.2(2)
O2 Co1 N2	131.01(5)	N4 Co1 N2	156.4(2)
O2 Co1 N1	91.90(5)	N5 Co1 N3	102.6(2)
N4 Co1 N2	132.70(5)	N5 Co1 N1	101.7(3)
N3 Co1 O1	92.12(5)	N5 Co1 N2	100.0(3)
N3 Co1 O2	131.94(5)	N5 Co1 N4	103.6(3)
N3 Co1 N4	80.11(5)	O1 N5 Co1	128.6(6)
N3 Co1 N2	81.82(5)		
N3 Co1 N1	132.65(5)		
N1 Co1 N4	81.36(5)		
N1 Co1 N2	79.64(5)		

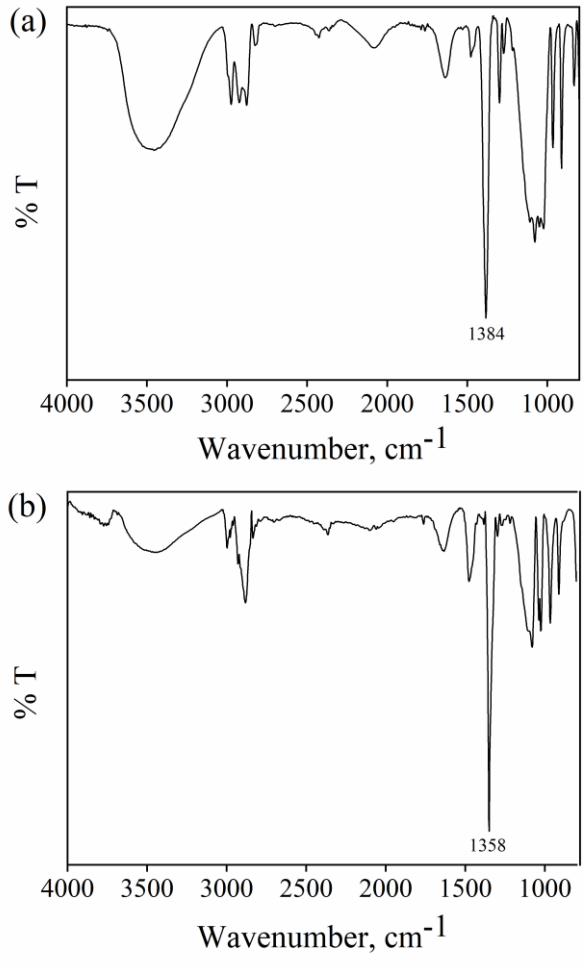

Figure. S1. FT-IR spectrum of (a) **2** recorded in KBr pellet at 298 K. The spectrum showed the peaks for aliphatic chain (2925 cm^{-1}), [Co-$^{14}NO_3^-$] (1384 cm^{-1}). (b) **2-**^{15} NO_3^- recorded in KBr pellet at 298 K. The spectrum showed peak [Co- NO_3^-] (1358 cm^{-1}).

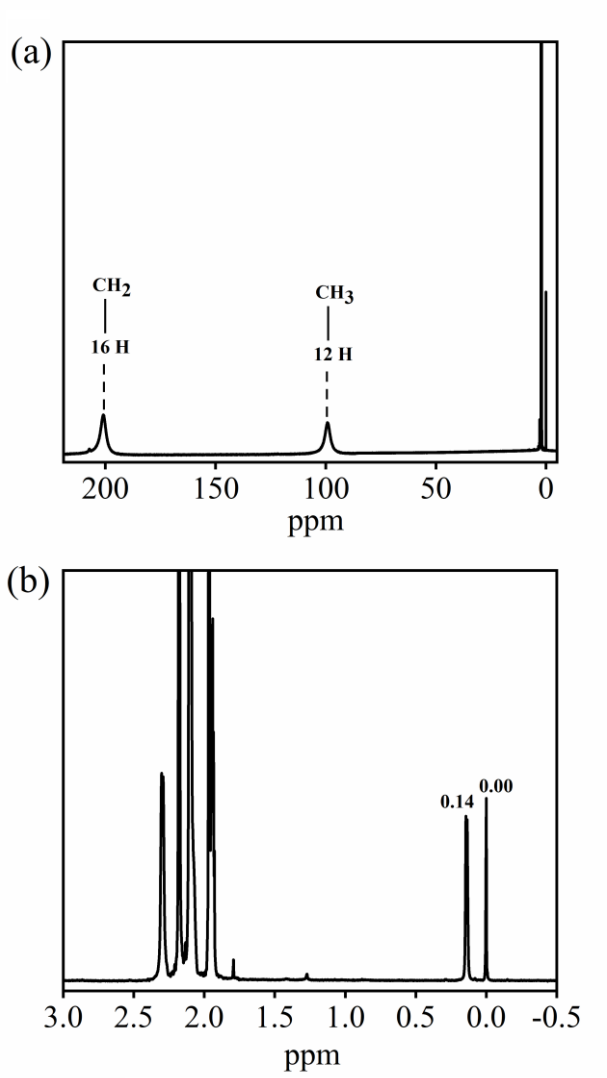

Figure S2. (a) Long range ^{1}H-NMR (400 MHz) spectra of complex **2** (4 mM) in CD_3CN. (b) ^{1}H-NMR (400 MHz) spectra of complex **2** (4 mM) in CD_3CN (0.1 % TMS), recorded in a coaxial NMR tube, with inside CD_3CN (1.0 % TMS) at RT.

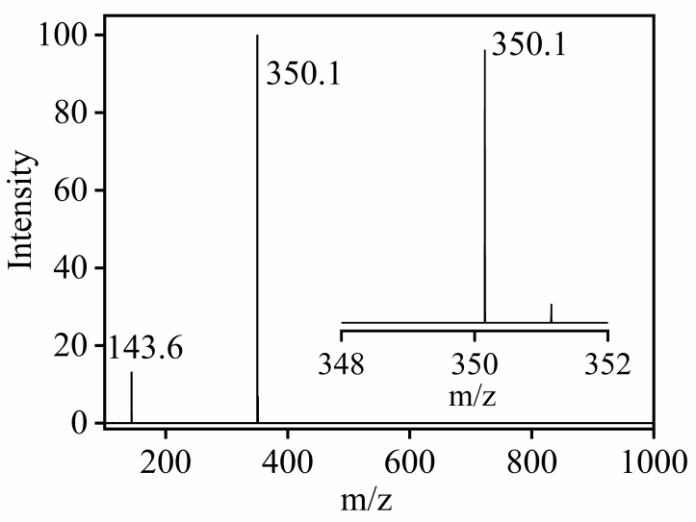

Figure S3. ESI-MS spectrum of **2-**$^{15}NO_3^-$, The peak at *m/z* 350.1 is assigned to be $[(12TMC)Co^{II}(^{15}NO_3)]^+$.

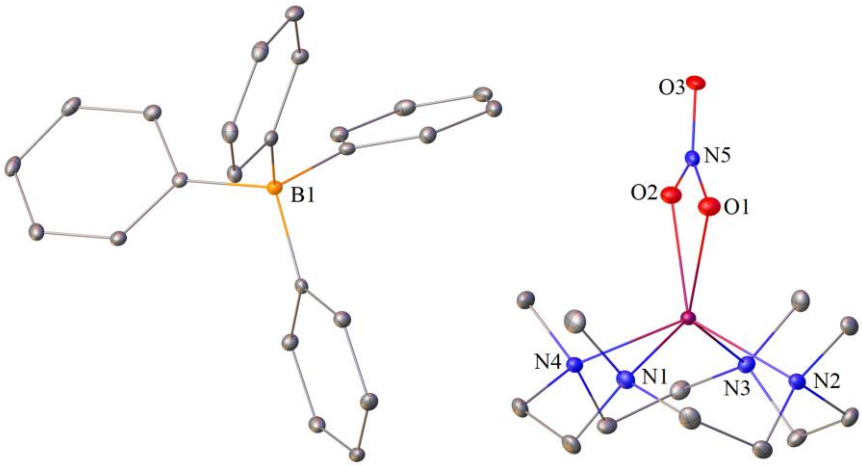

Figure. S4: Displacement ellipsoid plots of **2** with 20 % probability. Disordered C-atoms in the TMC ring and the H atoms have been removed for clarity

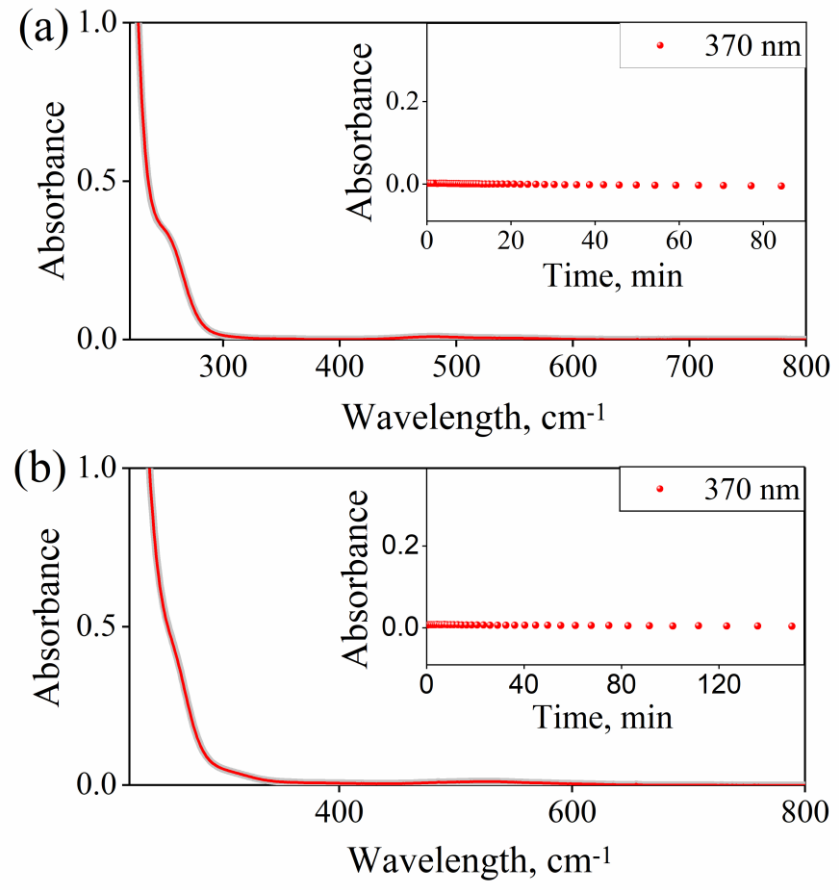

Figure. S5. UV-vis spectral changes of **2** (0.50 mM, Grayline to red line) in (a) H_2O (b) MeOH under Ar at 298 K. The Inset shows the time course of the natural decay of **2** (red circles) monitored at 370 nm in (a) H_2O (b) MeOH at 298 K.

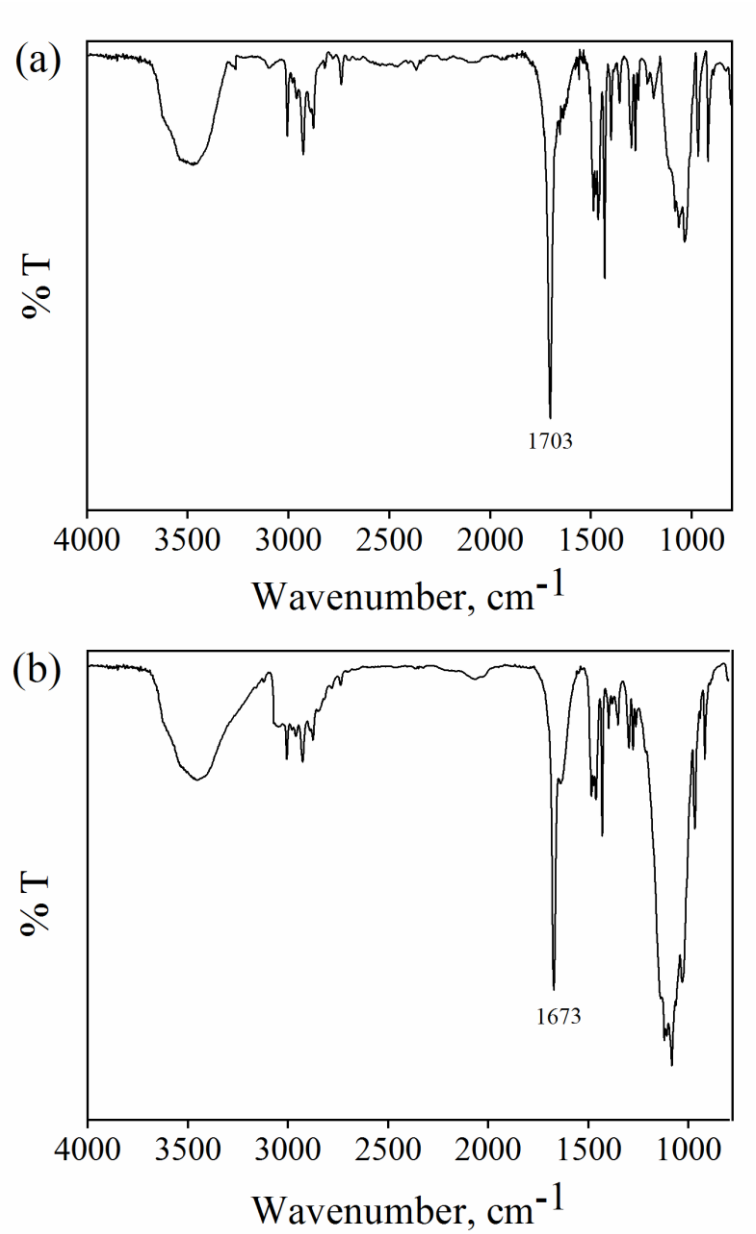

Figure. S6. FT-IR spectrum of (a) **4** isolated from the reaction of **2** + VCl_3 recorded in KBr pellet at 298 K. The spectrum showed the peaks for aliphatic chain (2925 cm^{-1}), [Co-^{14}NO] (1703cm^{-1}). (b) **4**-^{15}NO isolated from the reaction of **2**-^{15} NO_3^- + VCl_3 recorded in KBr pellet at 298 K. The spectrum showed the peaks [Co-^{15}NO] (1673 cm^{-1}).

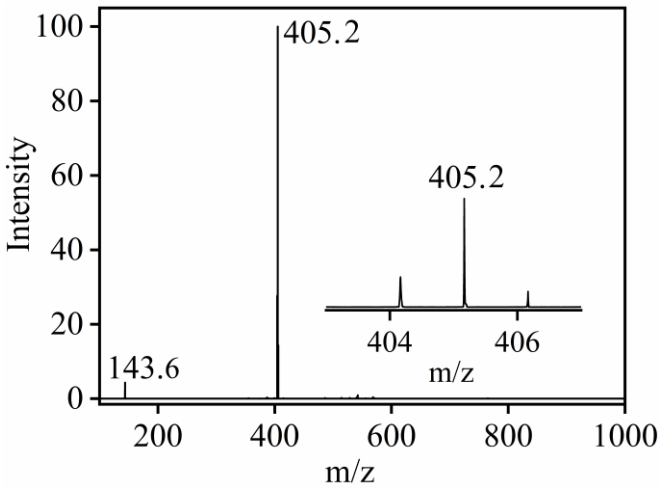

Figure S7. ESI-MS spectrum of **4**, formed in the reaction of **2-** $^{15}NO_3^-$ + VCl_3, in H_2O at 298K.

The peak at *m/z* 405.2 is assigned to be $[(12TMC)Co^{III}(^{15}NO)(BF_4)]^+$.

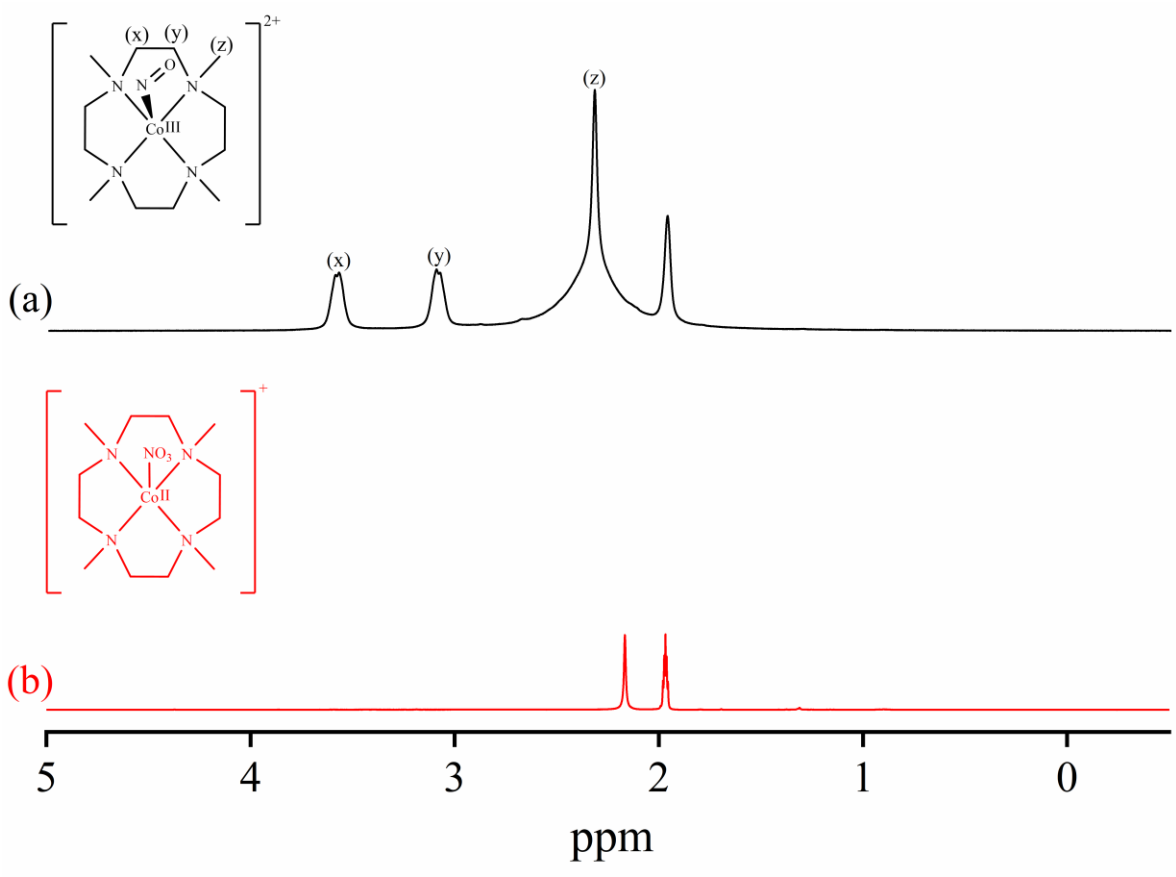

Fig. S8. ^{1}H-NMR (400 MHz) spectra of (a) isolated product from reaction of **2** + VCl_3 (**4**, 30 mM) and (b) complex **2** (30 mM).

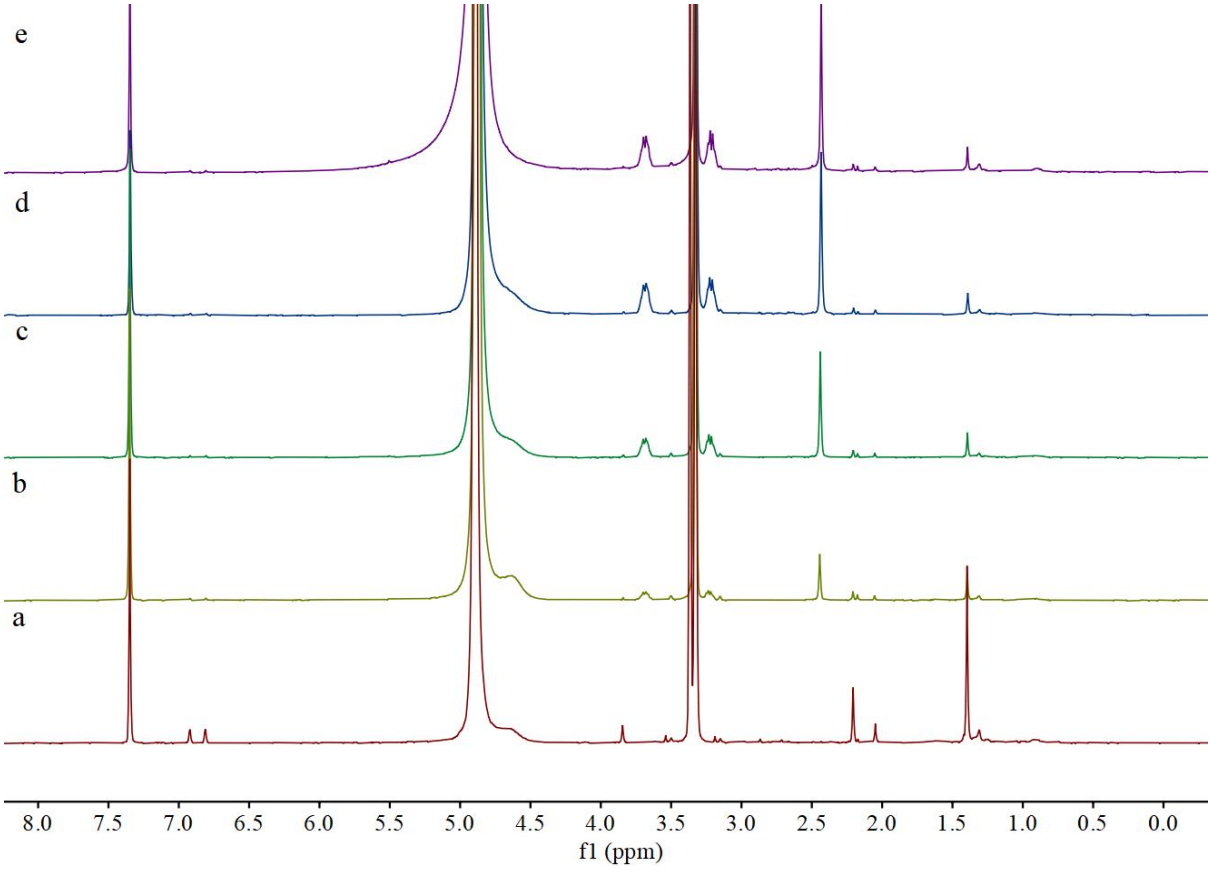

Fig. S9. ^{1}H-NMR (400 MHz) spectra of (a) complex **2** (4 mM), (b) complex **2** (4mM) and 0.2eq VCl_3 (0.8 mM), (c) complex **2** (4mM) and 1 equiv. VCl_3 (4 mM), (d) complex **2** (4mM) and 2.2 equiv. VCl_3 (8.8 mM), (e) complex **4** (4mM), benzene (4mM) as internal standard in CD_3OD.

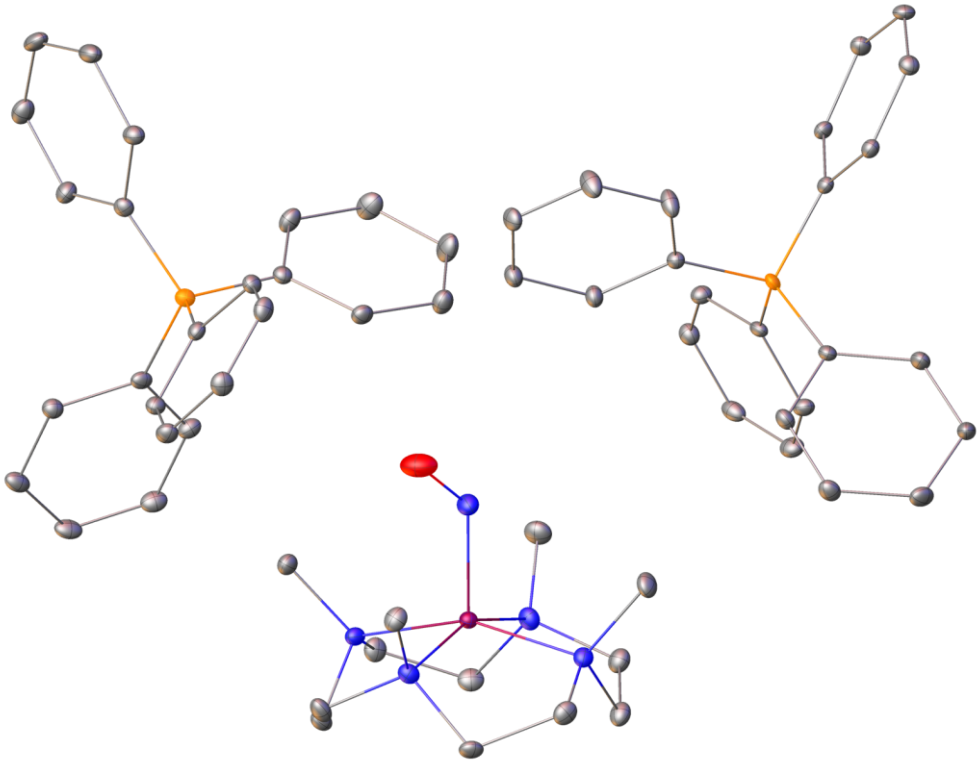

Figure. S10: Displacement ellipsoid plots of **4** with 20 % probability. Disordered C-atoms in the TMC ring and the H atoms have been removed for clarity

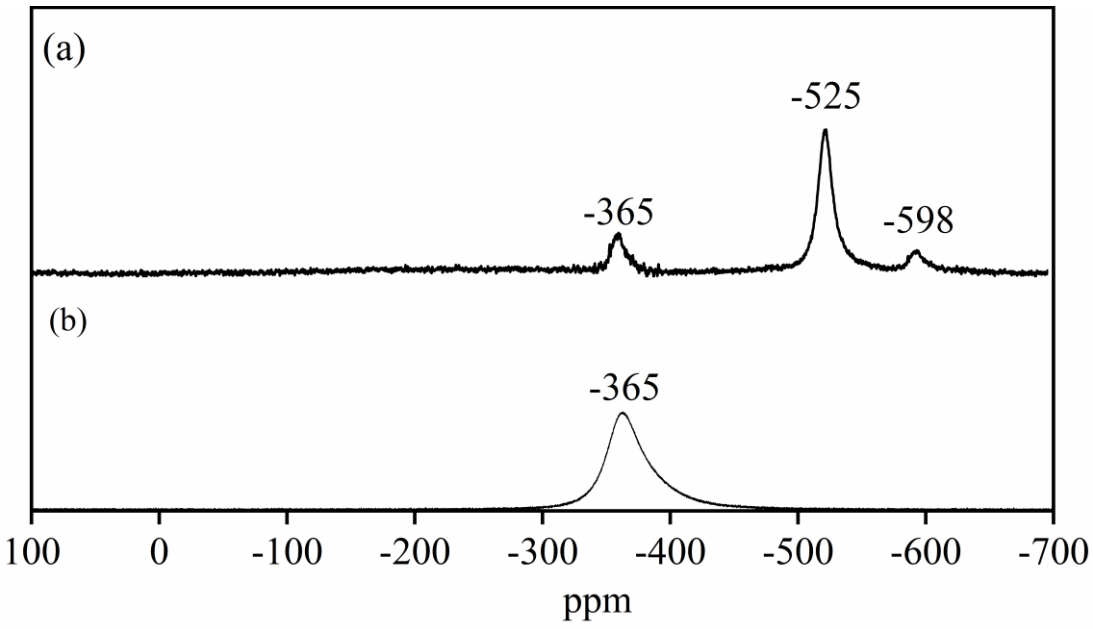

Fig. S11. ^{51}V-NMR (400 MHz) spectra of (a) reaction mixture **2** (15mM) + VCl_3 (35 mM) and (b) authentic sample of $VOCl_3$ (45 mM) in CD_3OD at RT.

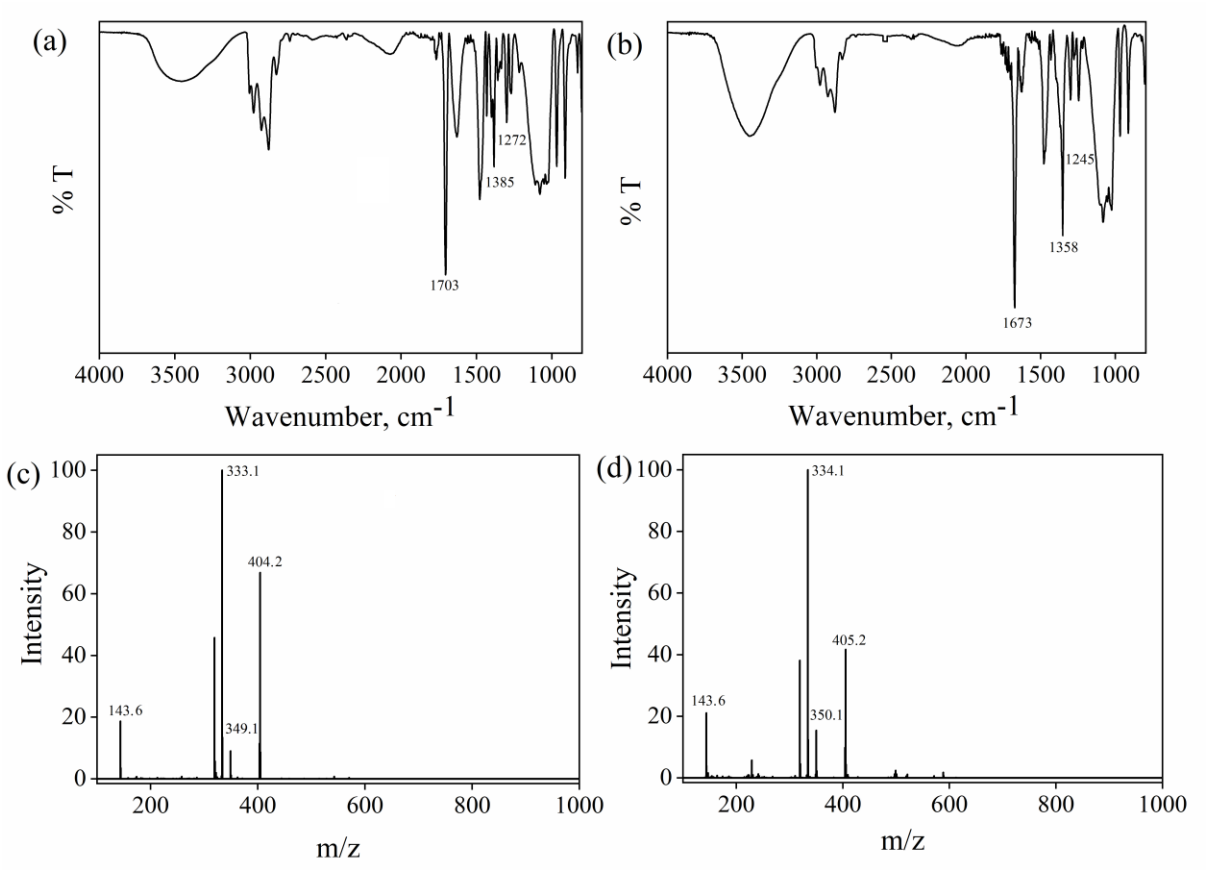

Figure. S12. FT-IR spectrum of (a) reaction mixture of **2** + 1equiv. VCl_3 recorded in KBr pellet at 298 K. The spectrum showed the peaks for aliphatic chain (2925 cm^{-1}), [Co-^{14}NO] (1703cm^{-1}), [Co-$^{14}NO_2^-$] (1272 cm^{-1}), [Co-$^{14}NO_3^-$] (1385 cm^{-1}). (b) Reaction mixture of **2**-$^{15}NO_3$ + 1equiv. VCl_3 showed the peaks for aliphatic chain (2925 cm^{-1}), [Co-^{15}NO] (1673cm^{-1}), [Co-$^{15}NO_2^-$] (1245 cm^{-1}), [Co-$^{15}NO_3^-$] (1358 cm^{-1}). (c) ESI-MS spectrum of reaction mixture, **2** + 1equiv. VCl_3, The peak at *m/z* 404.2, 349.1, 333.1 are assigned to be $[(12TMC)Co^{III}(^{14}NO)(BF_4)]^{2+}$, $[(12TMC)Co^{II}(^{14}NO_3^-)]^+$ and $[(12TMC)Co^{II}(^{14}NO_2^-)]^+$ respectively. (d) ESI-MS spectrum of reaction mixture, **2**-$^{15}NO_3$ + 1equiv. VCl_3 , The peak at *m/z* 405.2, 350.1, 334.1 are assigned to be $[(12TMC)Co^{III}(^{14}NO)(BF_4)]^+$, $[(12TMC)Co^{II}(^{14}NO_3^-)]^+$ and $[(12TMC)Co^{II}(^{14}NO_2^-)]^+$ respectively.

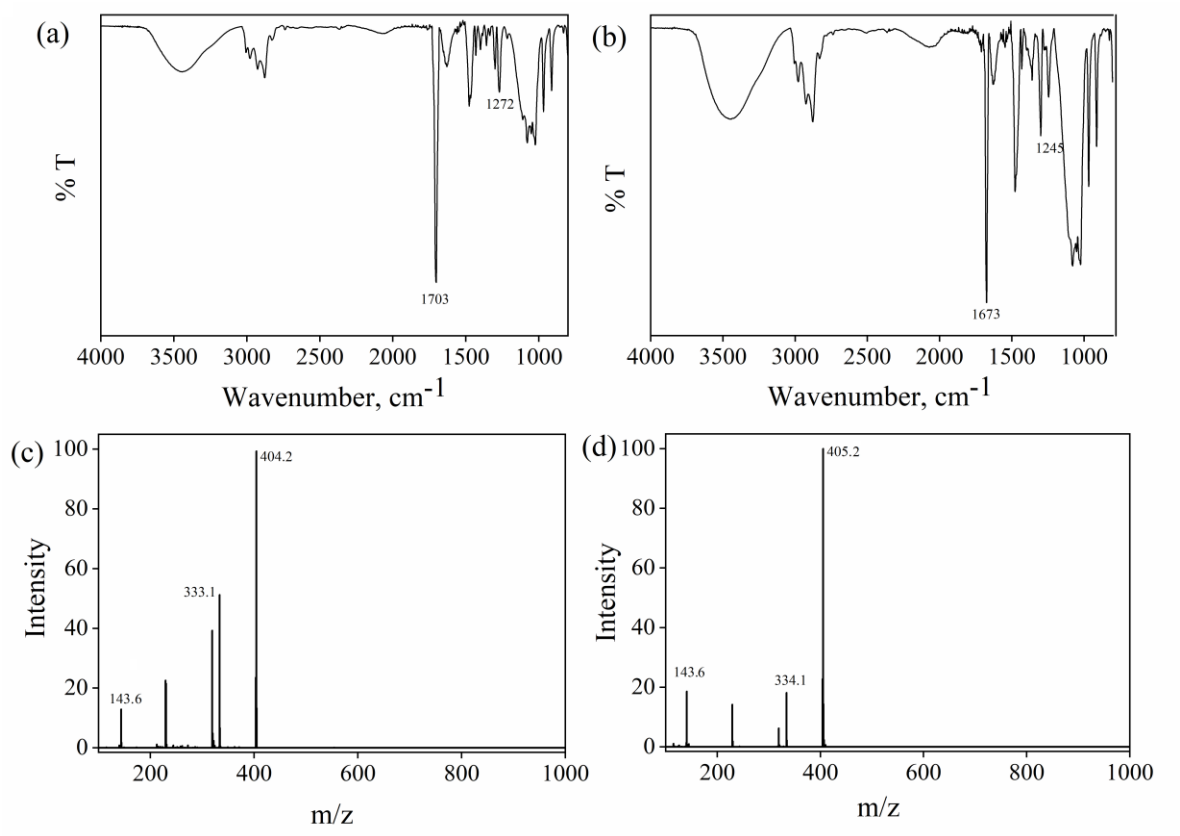

Figure. S13. FT-IR spectrum recorded in KBr pellet at 298 K of (a) reaction mixture of **2** + 1.5 equiv. VCl_3. The spectrum showed the peaks for aliphatic chain (2925 cm^{-1}), [Co-^{14}NO] (1703cm^{-1}), [Co-$^{14}NO_2^-$] (1272 cm^{-1}). (b) Reaction mixture of **2**-$^{15}NO_3^-$ + 1.5 equiv. VCl_3 showed the peaks for aliphatic chain (2925 cm^{-1}), [Co-^{15}NO] (1673cm^{-1}), [Co-$^{15}NO_2^-$] (1245 cm^{-1}). ESI-MS spectrum of reaction mixture, (c) **2** + 1.5 equiv. VCl_3, The peak at *m/z* 404.1, and 333.1 are assigned to be $[(12TMC)Co^{III}(^{14}NO)(BF_4)]^{2+}$ and $[(12TMC)Co^{II}(^{14}NO_2^-)]^+$ respectively. (d) **2**-$^{15}NO_3^-$ + 1.5 equiv. VCl_3, The peak at *m/z* 405.1, 334.1 are assigned to be $[(12TMC)Co^{III}(^{14}NO)(BF_4)]^+$ and $[(12TMC)Co^{II}(^{14}NO_2^-)]^+$ respectively.

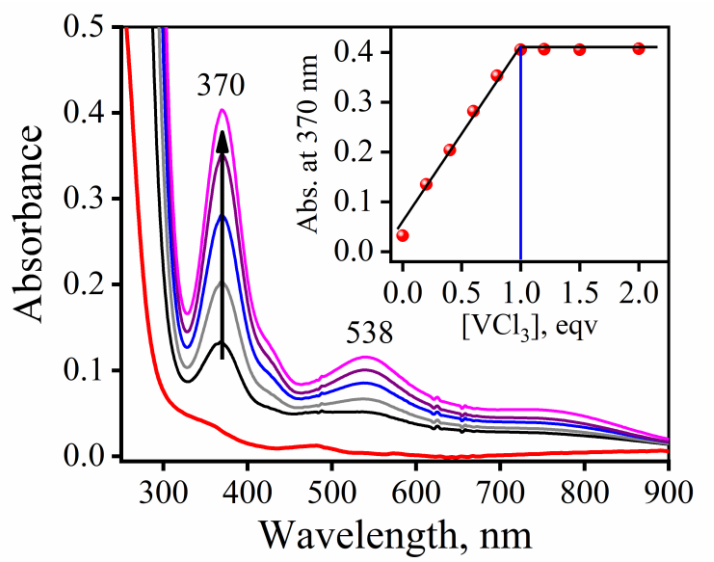

Fig. S14. UV-vis spectral changes observed in the reaction **3** with VCl_3 (in the increments of 0, 0.20, 0.40, 0.60, 0.8, 1.0, 1.2, 1.4, 1.6 equiv.) in H_2O under Ar at 298 K.

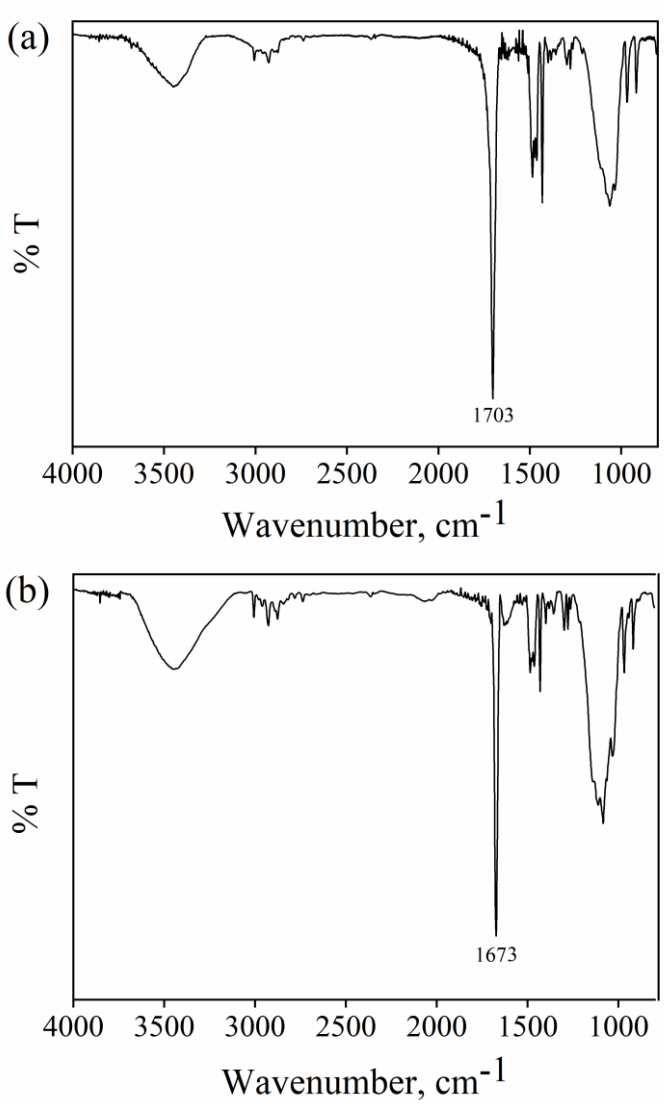

Figure. S15. FT-IR spectrum recorded in KBr pellet at 298 K of (a) isolated product of reaction mixture **2** + 1.1 equiv. VCl_3. The spectrum showed the peaks for the aliphatic chain (2925 cm^{-1}), [Co-^{14}NO] (1703cm^{-1}). (b) isolated product of reaction mixture **2**-$^{15}NO_2^-$ + 1.1 equiv. VCl_3. The spectrum showed the peaks [Co-^{15}NO] (1673 cm^{-1}).

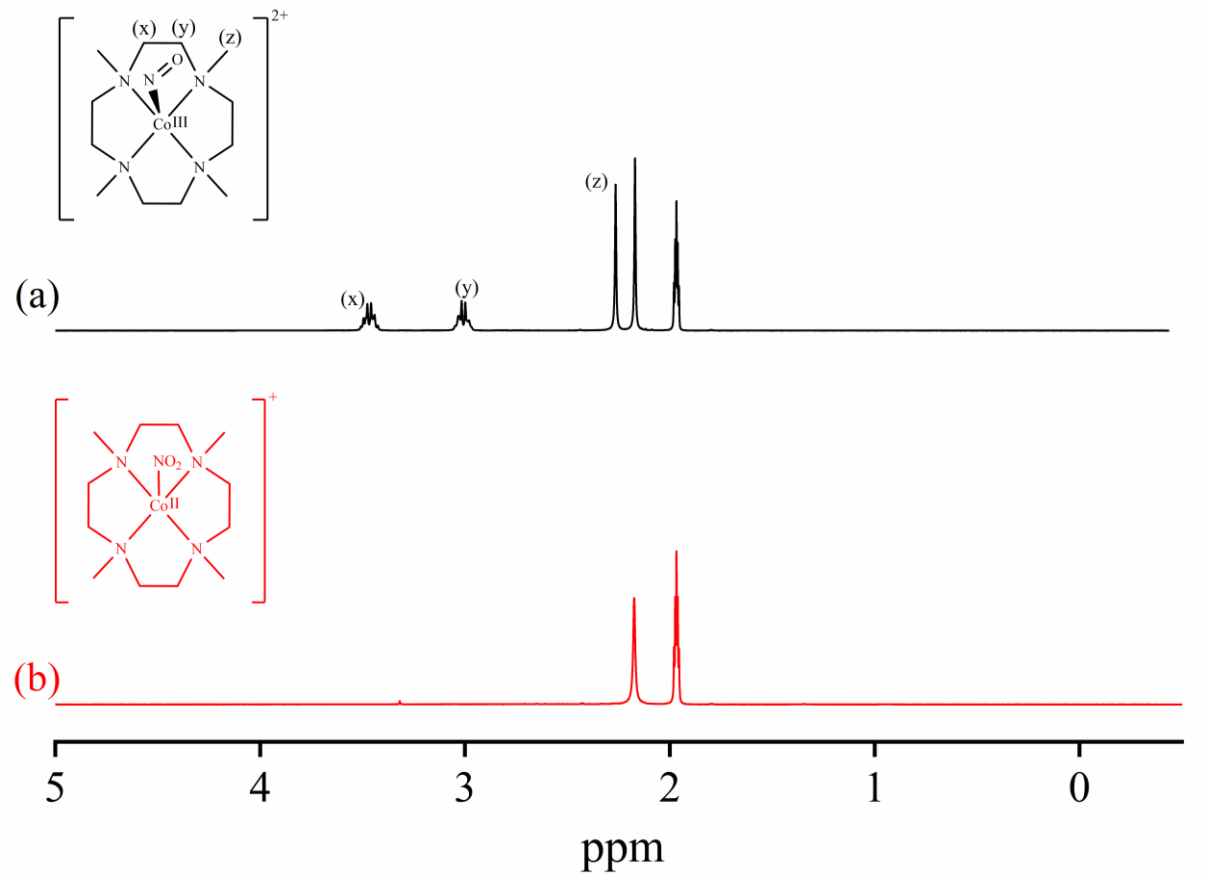

Fig. S16. ^{1}H-NMR (400 MHz) spectra of (a) isolated product from reaction mixture **3** (30 mM) + VCl_3 (30 mM) and (b) complex **3** (30 mM) in CD_3CN at RT.

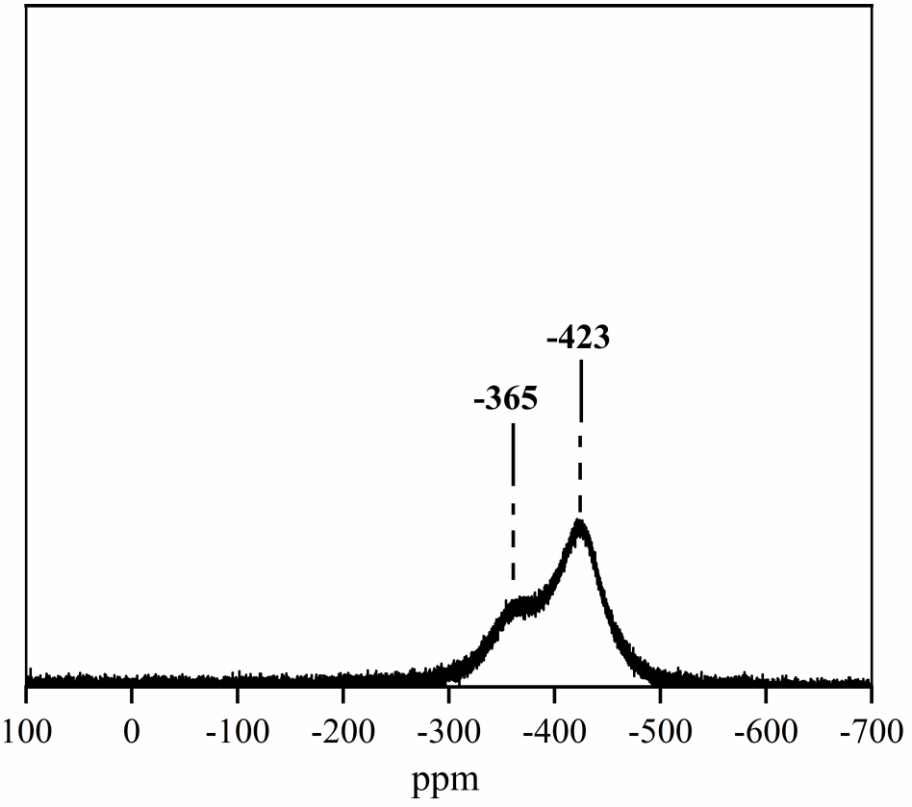

Fig. S17. ^{51}V-NMR (400 MHz) spectra of reaction mixture **3** + VCl_3

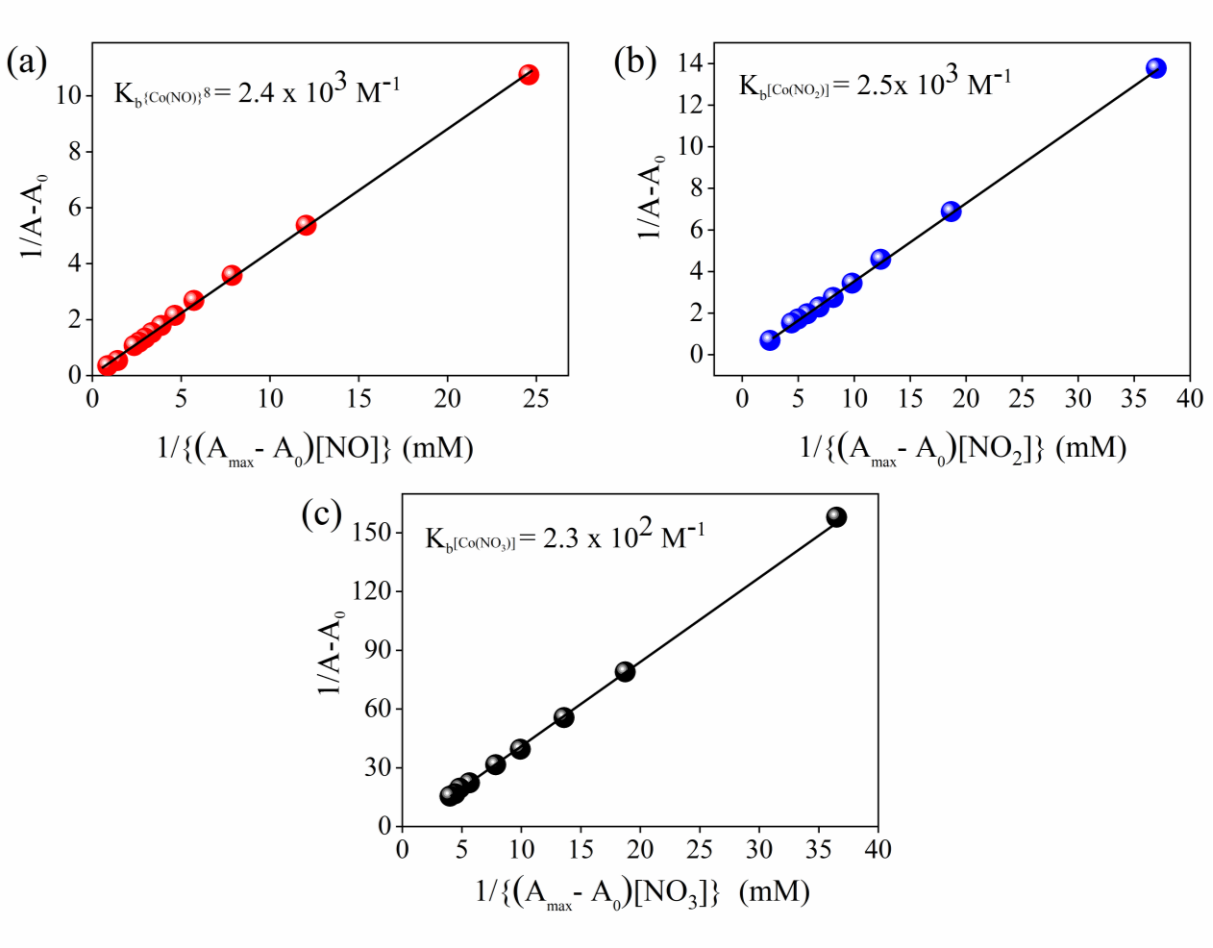

Fig. S18. Binding constants of complex (a) **4**, (b) **3**, (c) **2** calculated from the Benesi-Hildebrand equation.

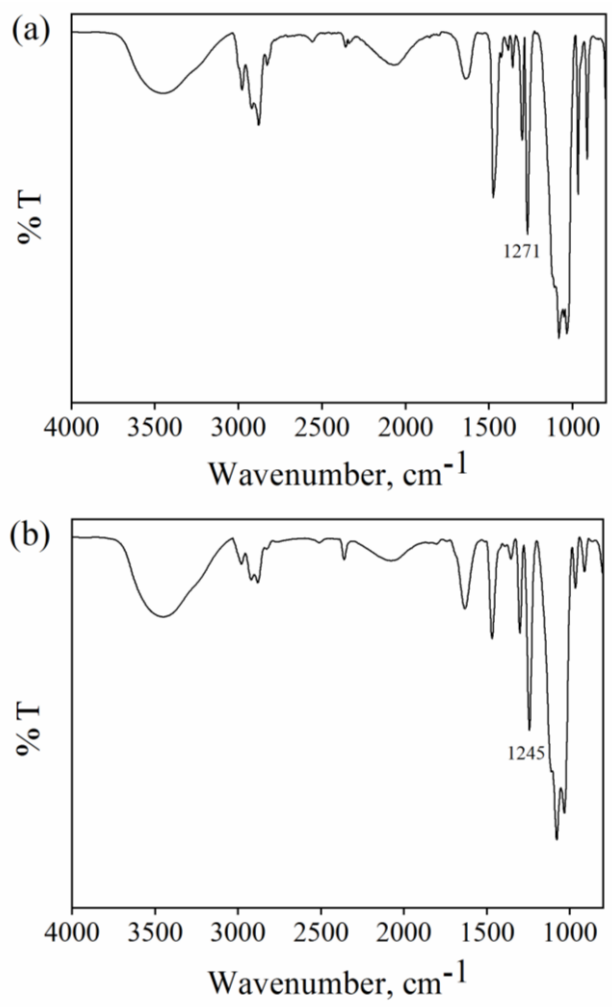

Figure. S19. FT-IR spectrum recorded in KBr pellet at 298 K of (a) complex **3**. The spectrum showed the peaks for the aliphatic chain (2925 cm^{-1}), [Co-$^{14}NO_2^-$] (1271 cm^{-1}). (b) **3**-$^{15}NO_2^-$. The spectrum showed the peaks [Co-$^{15}NO_2^-$] (1245 cm^{-1}).

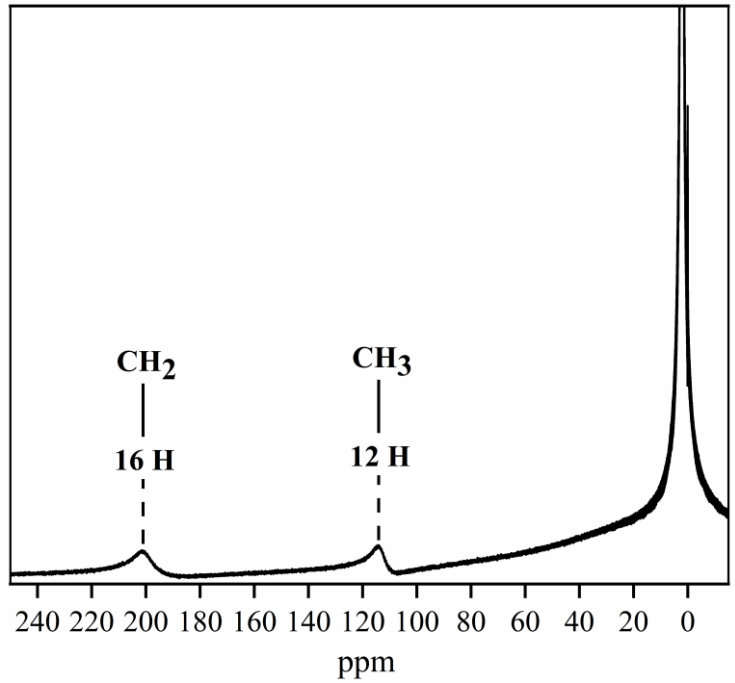

Figure. S20 Long range ^{1}H-NMR (400 MHz) spectra of complex **3** in CD_3CN.

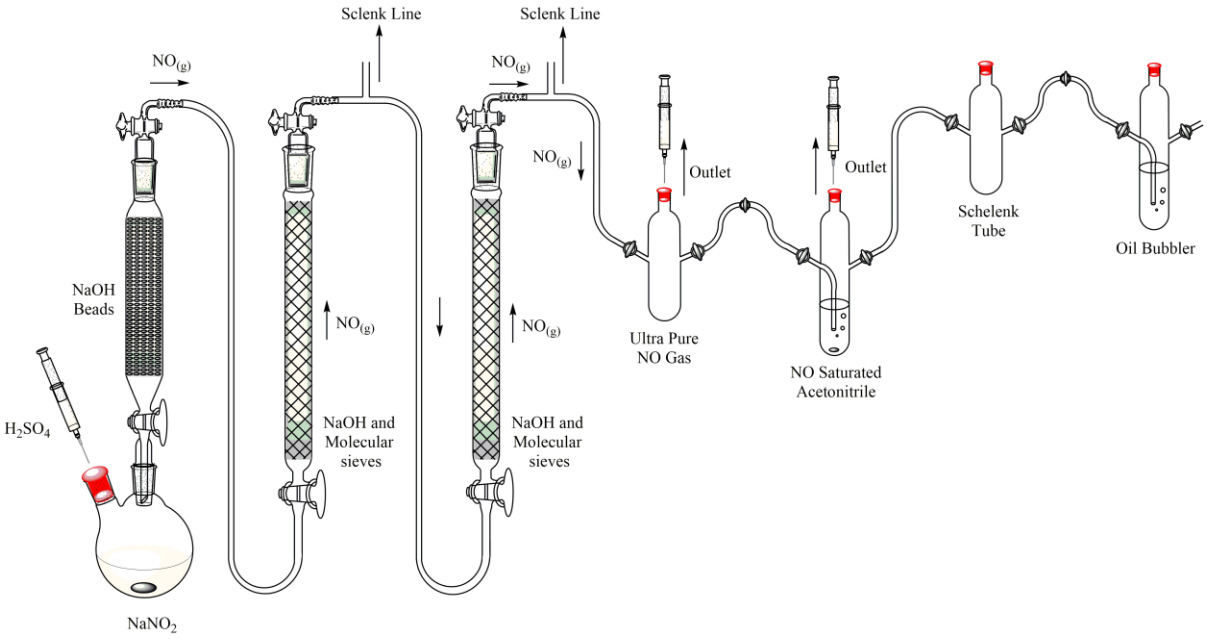

Fig. S21. Schematic diagram showing the generation and purification setup for NO.